Organic profiles of brake wear particles

Célia Alves, Margarita Evtyugina, Ana Vicente, Eleonora Conca, Fúlvio Amato

PII: S0169-8095(21)00109-5

DOI: https://doi.org/10.1016/j.atmosres.2021.105557

Reference: ATMOS 105557

To appear in: *Atmospheric Research*

Received date: 3 November 2020

Revised date: 9 February 2021

Accepted date: 24 February 2021

Please cite this article as: C. Alves, M. Evtyugina, A. Vicente, et al., Organic profiles of brake wear particles, *Atmospheric Research* (2021), https://doi.org/10.1016/j.atmosres.2021.105557

Organic profiles of brake wear particles

Célia Alves[1*], Margarita Evtyugina[1], Ana Vicente[1], Eleonora Conca[2,3], Fúlvio Amato[2]

[1]Department of Environment and Planning, Centre for Environmental and Marine Studies, University of Aveiro, 3810-193 Aveiro, Portugal

[2]Institute of Environmental Assessment and Water Research, Spanish Research Council (IDÆA-CSIC), 08034 Barcelona, Spain

[3]Department of Chemistry, University of Turin, Via Pietro Giuria, 10125 Turin, Italy

Abstract

Four brake pads were tested in a bench dynamometer under test cycles with different braking severities: i) two types of conventional brake pads (low steel 1 and 2), and ii) two types of non-asbestos organic brake pads (NAO 1 and 2) with non-ferrous materials. Wear particles (PM_{10}) were analysed for total carbon by a thermo-optical method and then solvent-extracted and analysed by gas chromatography-mass spectrometry. In general, the test protocols with less braking and lower temperatures gave rise to much lower PM_{10} levels. Total carbon accounted for PM_{10} mass fractions in a wide range (5.07-75.4%), generally decreasing with the severity of the braking cycles. More than 150 organic compounds were quantified, comprising aliphatics, polycyclic aromatic hydrocarbons (PAHs), alcohols, several types of acids (alkanoic, alkenoic, diacids and others), glycol/glycerol derivatives, plasticisers, sugars, sterols and several phenolic constituents. Globally, larger amounts of most of these compounds were emitted by NAO 2 under the smoothest braking cycle. Several correlations between compounds with the same functional groups were established. No PAH with five or more benzenic rings was detected. The differences in composition and concentrations are discussed based not only on the characteristics of the braking circuits, but also on the diverse quantities and types of organic compounds used in the brake pad formulations.

Keywords: brake wear, PM_{10}, PAHs, phenolic compounds, acids, plasticisers

Introduction

It is well known that on-road mobile sources are a major contributor to particulate matter (PM) emissions in urban areas (Amato et al., 2016; Cui et al., 2021; Mukherjee and Agrawal, 2018). Exhaust emissions of PM from road vehicles have been decreasing in recent years because of the effective implementation of various abatement technologies boosted by increasingly restrictive emission regulations. With the decline in exhaust emissions, non-exhaust sources, which are not currently controlled or regulated, became dominant. These non-exhaust emissions (NEE) include

* Corresponding author: celia.alves@ua.pt

particulate matter below 10 and 2.5 μm (PM_{10} and $PM_{2.5}$) arising from four sources: brake wear, tyre wear, road surface wear, and resuspended road dust.

According to UK inventories covering all primary emission sources (DEFRA, 2019), in 2000, NEE from brake, tyre, and road surface wear were 5.8% and 4.9% of total PM_{10} and $PM_{2.5}$ emissions, respectively, but these contributions have increased to 8.5% and 7.4% in 2016. It was reported that these three NEE contribute roughly similar amounts to the overall inventory and that there is no dominant source. By 2030, NEE are predicted to increase to 9.5% of total UK $PM_{2.5}$ emissions if no abatement measures are taken (DEFRA, 2019). By employing a combination of size-distribution measurements with chemical tracer information, Harrison et al. (2012) inferred that at London Marylebone Road the roadside increment in super-micron PM consisted of 55% of brake dust. A recent critical review of the scientific literature concluded that only a few articles explicitly provided an estimate of the contribution of brake wear to the ambient PM levels (FAT, 2017). As stated by this report, in the studies that did provide estimates, the contribution of brake wear ranged from around ~0.8 μg m^{-3} to 4 μg m^{-3} in busy urban roadside areas, accounting for about 5 to 10% of the PM_{10} mass. The literature shows that there are substantial uncertainties in estimating the contribution of brake wear to the atmospheric PM levels. Uncertainties stem from the fact that the composition of brake wear particles varies widely, and tracers thought to be unique, such as Cu and Sb, may also derive from other sources (FAT, 2017). Furthermore,
some of these metals are no longer used in pad formulations (Grigoratos and Martini, 2015).

Many studies focused on the characterisation of brake wear particles have been carried out in laboratories equipped with specific dynamometer benches (Garg et al., 2000; Hagino et al., 2016; Iijima et al., 2007, 2008; Kukutschová et al., 2010, 2011; Menapace et al., 2020; Mosleh et al., 2004; Sanders et al., 2003; Wahlström et al., 2010). All these studies provide extensive information on morphological characteristics and/or elemental composition of the particles generated by the abrasion processes. However, the organic composition has been completely neglected. As far as we know, only Rogge et al. (1993) analysed some organic constituents in brake lining dust (PM_2), but the information provided refers to only one sample. Brakes pads are composed of many different and often complex and unknown formulations. There are many brands of brake components on the market, comprising fillers, binders, reinforcing agents (fibres) and friction modifiers (abrasives and lubricants) (Thorpe and Harrison, 2008). While the filler and fibre components are mostly metallic, additives and binders are, in general, carbonaceous materials (Blau, 2001; Grigoratos and Martini, 2015; Gudmand-Høyer et al., 1999; Sanders et al., 2003; Thorpe and Harrison, 2008; Xiao et al., 2016).

During the braking process, friction between the pad and disc surfaces is employed to convert the vehicle kinetic energy into heat. Consequently, a substantial alteration of the lining components and a temperature rise take place (Kukutschová et al., 2011). Depending on the driving conditions, the temperature can rise ~~up~~ to 400 °C and locally it can even attain values up to 700-1000 °C (Garg et al., 2000; Iijima et al., 2008; Sokolski and Sokolska, 2019). Frequently depicted as coarse mode PM,

brake wear debris also exist within the respirable fine and ultrafine fractions (Grigoratos and Martini, 2015; Hagino et al., 2016; Iijima et al., 2008; Kukutschová et al., 2010, 2011; Mamakos et al., 2019; Sanders et al., 2003), so they can penetrate deeply into the airways. After reaching the alveolar region, these particles may cross the air-blood barrier and accumulate in secondary organs (Ciudin et al., 2014). In fact, during braking at high temperatures, metallic particles in the nano- to micrometre range are produced, jointly with carbon-based particulates resulting from the condensation of evaporated organic compounds (Kukutschová et al., 2011). So far, few studies have dealt with the toxicity of brake wear particles (Barosova et al., 2018; Gasser et al., 2009; Gerlofs-Nijland et al., 2019; Kazimirova et al., 2016; Malachova et al., 2016; Selley et al., 2020; Zhao et al., 2015). It has been observed that these particles have the potential to induce inflammatory responses via oxidative stress and other mechanisms.

The organic composition of brake wear particles should be considered when assessing their possible adverse effects on human health. Moreover, to improve source apportionment models, such as the Chemical Mass Balance, speciated organic profiles are necessary. This study is one of the first attempts of providing a comprehensive organic characterisation of wear particles from different brake brands.

Methodologies

Sampling

In this study, different types of brake pads were tested in a bench dynamometer with the brake system closed in an environmental chamber. The chamber contains the entire front wheel with a disc and a calliper, as well as a wind tunnel simulating the airflow. The brake pads have been manufactured with the following general composition:

- phenolic resins (5-10%)
- aramid fibre (1-5%)
- lubricants: graphite (1-5%); metal sulphides (1-10%)
- oxides: Ca/Mg/Al/Si/Zr (1-15%)
- metals: Cu/Fe (fibres/powder) (0-30%)
- others: barite, chromite, aluminosilicates (10-30%)

The brake pads can be grouped as follows: i) conventional brake pads (low steel) commonly used in the European market; ii) non-asbestos organic brake pads (NAO) with non-ferrous metals, typical of the USA. Two types of brake discs were tested for each one of these two categories. However, it is not possible to provide full compositional details for the distinct types, because brake materials are proprietary formulations. Different cycles have been followed: a) the smoothest protocol - 8 braking events, 120-80 kph deceleration, temperature 100 ºC; b) protocol similar to the previous one but with

higher speeds - 8 braking events, 200-170 kph deceleration, temperature 100ºC; c) an additional cycle (FADE), with more severe braking and higher temperature and pressure, comprising 15 braking events, 100-5 kph deceleration, maximum temperature 550 ºC.

Pallflex 47 mm diameter Tissue Quartz 2500 QAT-UP filters were used to collect PM_{10} samples at a flow of 10 L min^{-1}. Before and after sampling, the quartz microfibre filters were conditioned for 48 h at 20 ºC and 50% relative humidity. The weights of the filters were obtained gravimetrically in a microbalance (1 µg sensitivity).

Analytical techniques

Total carbon (TC) was determined using a thermo-optical transmittance method, following the EUSAAR-2 temperature program, by means of a laboratory Sunset instrument. Due to the high iron content in brake wear particle emissions, it was not possible to carry out the separation between organic carbon and elemental carbon. In fact, iron oxide can oxidise some elemental carbon under intense heat, compromising the correct split between organic and elemental carbon.

Samples available for organic speciation are listed in Table 1. Given that part of the filters was subjected to other type of analyses that do not constitute the target of the present study, and due to the need to repeat some determinations, it is not possible to present the organic composition of particles from all brake pads for all braking cycles, because there was no filter left.

Table 1. PM_{10} samples from brake wear available for organic speciation

Filter Ref.	Brake pad	Braking cycle
A	NAO 1	120-80 kph
B	NAO 1	200-170 kph
C	NAO 2	120-80 kph
D	NAO 2	200-170 kph
E	Low Steel 1	120-80 kph
F	Low Steel 1	200-170 kph
G	Low Steel 2	120-80 kph
H	Low Steel 2	FADE

The quartz filters were consecutively extracted with dichloromethane and methanol. After filtration of both solvents, the combined organic extract was concentrated to a volume of 0.5 mL in a TurboVap® evaporator workstation and then dried under a gentle nitrogen stream. Flash vacuum column chromatography was used to separate the extracts into five groups of organic compounds using eluents of increasing polarity. Prior to speciation by gas chromatography-mass spectrometry (GC-MS), the extracts with oxygen-containing functional groups were derivatised to trimethylsilyl ethers (TMS). The TMS derivatives were analysed in a GC-MS from Thermo Scientific (Trace Ultra,

quadrupole DSQ II) equipped with a TRB-5MS 60 m × 0.25 mm × 0.25 μm column. Aliphatic and polycyclic aromatic hydrocarbons (PAH) were determined in a Shimadzu QP5050A equipped with a TRB-5MS 30 m × 0.25 mm × 0.25 μm column. Six deuterated compounds (acenaphthene-d_{10}, chrysene-d_{12}, 1,4-dichlorobenzene-d_4, naphthalene-d_8, perylene-d_{12}, and phenanthrene-d_{10}) contained in the EPA 8270 semi-volatile internal standard mix (Supelco), benzo[a]pyrene-d12 (Supelco) and fluorene-d_{10} (Aldrich) were used to spike the PAH extracts. Extracts from other functional groups were spiked with 3 internal standards (1-chlorohexadecane and 1-chlorododecane, both from Merck, and tetracosane-d50, from Aldrich). Around 200 authentic standards in different concentration levels were used to perform multipoint calibrations. Data were acquired in both full scan and selected ion monitoring (SIM) modes. Additional details of the analytical methodology can be found elsewhere (Alves et al., 2011).

Results and Discussion

Particle and total carbon levels

Particle concentrations varied substantially depending on the type of brake pads and test cycle (Table 2). The highest values were obtained for the FADE circuit, which includes 15 braking steps, and the pads reach temperatures above 500º C. Thus, besides mechanical emissions due to wear and tear, it is likely that some of the brake pad materials volatilise during braking and condense in the airstream, contributing to ultrafine particle formation. The two test protocols with less braking and lower temperatures gave rise to much lower levels (up to almost 2 orders of magnitude). Except for low steel 2 brake pads, the lowest particle concentrations were produced during the test runs involving lower braking pressures. The results indicated that the lowest particle levels were generated by NAO brake pads, for the two less severe protocols, while the peak concentrations were associated with the conventional European (low steel) pads.

Total carbon accounted for PM_{10} mass fractions in a wide range (5.07-75.4%). In general, the carbonaceous content decreased with the severity of the braking cycles. The highest mass fraction of TC was obtained in PM_{10} emitted by NAO 1 brake pads during runs with less braking and lower temperature. Hagino et al. (2016) tested two passenger cars (vehicles I and II) and one middle-class truck (vehicle III) using a dynamometer system under urban city driving cycles to evaluate airborne brake wear particle emissions. TC accounted for 7.3, 7.9 and 41%, respectively, of the PM_{10} produced during the friction tests. The mass fractions of this carbonaceous component were found to be lower than ~~the~~ 21% and 17% for 100 ºC and 300 ºC tests by Garg et al. (2000), suggesting variations in the amount and ratio of TC from airborne PM caused by differences in brake friction and temperature. Since the carbon contents of the pads and linings were semi-quantified as 37, 34, and 6%, for vehicles I, II, and III, respectively, Hagino et al. (2016) suggested that parts of the carbon components are

volatilised and/or oxidised. Malachova et al. (2016) characterised four types of samples: i) two commercial low-metallic automotive brake pads (sieved samples I and II < 200 µm) used by some manufacturers in the EU, ii) a model brake pad with known formulation resembling a typical "low-metallic" friction material, iii) brake wear particles (non-airborne wear debris) generated by a simulation of various braking scenarios in ~~the~~ a dynamometer test, and iv) phenolic resin and antimony trisulfide representing two components that are frequently used in the formulation of friction materials. Total carbon represented mass fractions of 25.2, 18.5, 49.0 and 41.1%, respectively. Hussain et al. (2014) characterised by scanning electron microscopy with energy-dispersive X-ray spectroscopy the debris from NAO and semi metallic brake pads collected in a test rig. The carbon content accounted for 17.6 and 20.9%, respectively, of the wear particles. Attention is drawn to the fact that comparisons between studies must be made with due care, since the particulate material can represent different braking cycles and size ranges (airborne versus bulk debris) and have been subjected to different analytical techniques.

Table 2. PM_{10}, total carbon and particle carbonaceous mass fractions for different pads under distinct braking cycles

Braking cycle	120-80 kph			200-170 kph			FADE		
Brake pads	PM_{10} mg m^{-3}	TC µg m^{-3}	TC/PM_{10} %	PM_{10} mg m^{-3}	TC µg m^{-3}	TC/PM_{10} %	PM_{10} mg m^{-3}	TC µg m^{-3}	TC/PM_{10} %
NAO 1	0.301	227	75.4	0.768	298	38.8	26.0	1752	6.74
NAO 2	0.311	169	54.3	1.42	175	12.3	17.2	1394	8.10
Low steel 1	1.25	182	14.6	1.38	190	13.8	11.9	n.a.	n.a.
Low steel 2	3.35	170	5.07	1.58	217	13.7	11.4	753	6.61

n.a. – not available

Organic speciation

During forced deceleration, brake linings are subject to large frictional heat generation and abrasion, leading to the formation of wear particles. Because brake linings must resist to extreme mechanical and heat stress and to possible brake fluid leak, organic fibres and binders are employed, which have a high boiling point and low solubility in solvents. Thus, only a small fraction of the organic content of wear particles can be chromatographically resolved. The identifiable organic fraction of PM_{10} samples consisted of *n*-alkanes, PAHs, phenolic compounds, aliphatic alcohols, sterols, polyalkylene glycol ethers, carboxylic and dicarboxylic acids, phthalates, among others (Table S1).

The extractable portion of brake wear particles comprised *n*-alkanes from C_{11} to C_{33}. A clear difference in the total mass fractions between the FADE protocol (62.5 µg g^{-1} PM_{10}) and the remaining test cycles (4.54-68.1 mg g^{-1} PM_{10}) was registered (Figure 1), suggesting that severe braking, high temperatures and pressures can cause degradation of these aliphatic compounds. Very good relationships between the particle mass fractions of most individual n-alkanes > C_{20} and the total mass fractions of these aliphatic constituents were obtained (Table S2), pointing to the possibility of using these predictive equations when it is not possible to quantify all compounds. The carbon preference index (CPI) has been widely used as an indicator of the organic matter input. For hydrocarbons derived predominantly from mature crude oil or derivatives, the CPI value approaches 1, while compounds from terrestrial sources (e.g. plant waxes) and/or at low maturity exhibit a predominance of odd-numbered alkanes, resulting in a high ratio. Except for NAO 1 brake wear particles, for which the CPI calculation does not make sense due to the great discontinuity in the homologous series, a rather constant ratio around 1 was obtained (0.99±0.17), suggesting the incorporation of mature petroleum products in brake pad formulations.

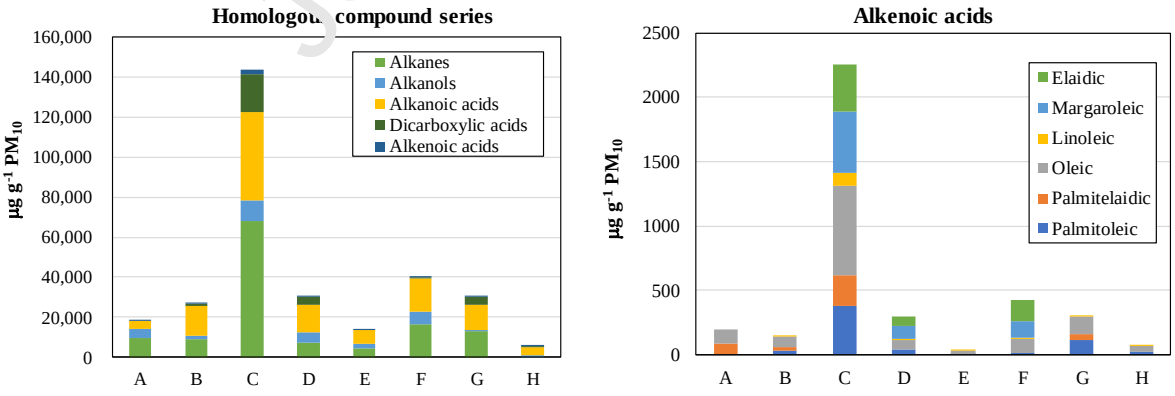

Figure 1. Particulate mass fractions of homologous series of various groups of organic compounds (A to H refer to different brake pads and test protocols, as listed in Table 1).

The aliphatic fraction also encompassed some alkenes, among which the most frequent were tetradecene, hexadecene and octadecene. As observed for n-alkanes, the total mass fractions for the FADE braking cycle were comparatively much lower (13.2 µg g^{-1} PM_{10}) than those recorded for the other tests (35.5-1242 µg g^{-1} PM_{10}). Except for low steel 1 pads, the highest mass fractions were associated with emissions from the smoothest braking circuit. An excellent correlation (y=0.018x+12.5, r^2=0.96) between total n-alkanes (x, µg g^{-1} PM_{10}) and total n-alkenes (y, µg g^{-1} PM_{10}) was derived, suggesting common emission pathways.

Trace amounts of PAHs were detected in PM_{10} samples (Figure 2). The brake pads NAO 1 and NAO 2 showed completely different PAH emission patterns. While, in the first case, no polyaromatics were detected for the smoothest braking cycle, in the second case, the highest PAH particulate mass fraction was produced among all samples for the same test run. As observed for n-alkanes, some PAHs correlated to each other, also presenting good relationships with the total mass fractions in the particulate material (Table S3). These compounds are likely formed during the heat build-up when braking. The temperatures of several hundred ºC sometimes reached (Iijima et al., 2008; Sokolski and Sokolska, 2019) can contribute to the pyrolysis of some organic components of the brakes. Regardless of the sample, no PAH with 5 or more benzene rings was detected. Malachova et al. (2016) made a GC-MS screening of dichloromethane extracts of the sieved fraction of two ball milled commercial low-metallic automotive brake pads reporting the presence of PAHs up to 5-benzenic rings in only one sample, while these compounds were completely absent from the other sample. This suggested that, although the brake pads fall into the same category, they could contain significantly different organic materials. When compared to the milled brake pads, the non-airborne wear debris resulting from braking simulations encompassed a markedly lower number of organic constituents. The researchers raised the hypothesis of weight loss due to temperatures above 100 ºC achieved during braking.

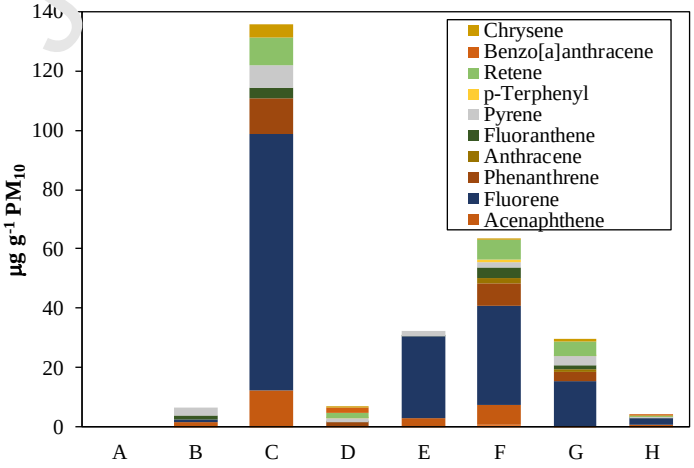

Figure 2. Particulate mass fractions of polycyclic aromatic hydrocarbons (A to H refer to different brake pads and test protocols, as listed in Table 1).

Except for NAO 1 brake pads, retene was detected in all the remaining samples. This alkylated phenanthrene has been proposed as a molecular marker of coniferous wood combustion (Ramdahl, 1983). However, recently, it has been reported as a constituent of both road dust (Alves et al., 2020a) and wear particles from the interaction between tyres and pavements (Alves et al., 2020b). Its detection in brake wear particles is probably related to the use of natural waxes and resins in the list of ingredients of this vehicle component. In the same samples, the presence of 9H-carbazole was also detected. This aromatic heterocyclic compound occurs in emissions of all incomplete combustion processes of nitrogen-containing organic matter (Fromme et al., 2018). It should be noted that nitrile rubber and paramid fibres are organic materials that are usually part of the composition of the brakes, so they can be the source of carbazole emissions.

A discontinuous series of n-alkanols was detected in the PM_{10} samples. The most abundant homologous compound was heptadecanol with PM_{10} mass fractions ranging from 182 µg g^{-1} to 5.15 mg g^{-1}, which accounted for 19-76 % of the total levels of this organic class. For both NAO brake pads, the total amounts of n-alkanols emitted were 2 to 5 times higher for the smoothest protocol compared to the most severe braking cycle. The mass proportions in the particulate material resulting from the wear of low steel 2 were much lower than those found for other types of brake pads.

Contrarily to what was reported by Rogge et al. (1993), who analysed the PM_2 fraction of dust retained in the rear drum brakes of a light truck, in the present study, palmitic (C_{16}) and stearic (C_{18}) acids were the most abundant homologues found in PM_{10} from brake wear, while low molecular weight *n*-alkanedioic acids were also representative, but not dominant. The homologous series o n-alkanoic acids comprised compounds between C_8 and C_{22}. Palmitic acid was present in all samples at mass fractions in the range 0.827-11.9 mg g^{-1} PM_{10}, representing 20 to 77% of the total amounts of n-alkanoic acids. With the exception of wear particles generated from NAO 1 brake pads during the smoothest braking protocol, stearic acid was also detected in all samples (1.93-15.5 mg g^{-1} PM_{10}), accounting for 28-50% of the total levels of this class of acids. Globally, the highest mass proportions of n-alkanoic acids were registered for PM_{10} from the wear of NAO 2 brake pads. Most acids correlate with each other and have good relationships with global amounts (Tables S4 and S5), indicating a similar origin or formation process and the possibility of using these linear equations as predictors of the concentrations of other homologues.

Some C_{16}, C_{17} and C_{18} alkenoic acids were also detected in the PM_{10} samples. The most abundant and always present, irrespective of the brake type or test protocol, was oleic acid (34.9-694 µg g^{-1} PM_{10}). Dicarboxylic acids, from ethanedioic to decanedioic, were identified in wear particles, as well. However, while they were relatively abundant in samples from NAO 2 brake pads, no homologue was found in samples from NAO 1 and low steel 1 under the smoothest braking protocol. Some hydroxy- and ketoacids were also present, following the abundances observed for diacids.

Various plasticiser constituents were observed in the PM_{10} from brake wear (Figure 3). Globally, the greatest amounts were found in samples from NAO 2. Regardless of the brake pads or test protocol, di-n-butyl phthalate was always present. In a study focused on sampling specific products and waste known or suspected to be a source of plasticiser contamination in stormwater, high concentrations of bis(2-ethylhexyl) phthalate, di-n-butylphthalate, butylbenzyl phthalate and diethyl phthalate were found in brake pads and brake pad dust (Dale and Trim, 2017). A brake lining for a disc brake, with a lining carrier and a friction lining, is designed such that the lining carrier has a rigid core which partially extends into a layer forming a plate on at least one side. Generally, this plate consists of a plasticised material to embed the core.

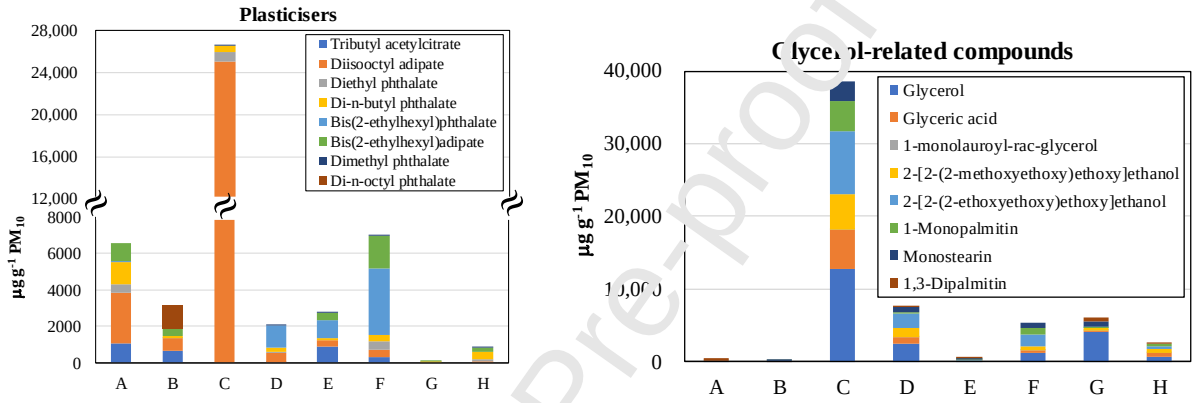

Figure 3. Particulate mass fractions of plasticiser and glycerol-related compounds (A to H refer to different brake pads and test protocols, as listed in Table 1).

Many glycol and glycerol-related compounds were among the constituents of brake wear particles. Once again, the highest abundances were obtained in PM_{10} from NAO 2 brake pads. Since many organic compounds are cytotoxic, higher concentrations may pose greater health risks. To confirm this hypothesis, organic extracts from all samples are being subjected to various lung cell line-based bioassays for toxicological evaluation. The results will be reported in an upcoming publication. Like glycol, glycerol has also been used as a base substance for the production of hydraulic brake fluids (Eze, 2016). Polyalkylene glycol ethers are the most common ingredients of these fluids. They have been previously detected as abundant compounds in the solvent-extractable organic fraction of brake lining debris (Rogge et al., 1993) and in road dust PM_{10} samples (Alves et al., 2018).

A long list of phenolic compounds was found in the particulate matter from wear of brake disks (Table 3). Globally, the highest amounts of these constituents were emitted by both NAO brake pads during the smoothest braking cycle. Benzyl alcohol and 2,4-di-tert-butylphenol were the two most representative phenolic compounds. Gadd and Kennedy (2000) inspected six different commercial brake pads and found phenolic compounds to be the most abundant species in organic extracts. Many phenolic resins are used as binders for friction materials which are employed for brake linings, disc

brake pads, clutch plates of transmission and others, offering heat resistance and adhesive performance. Since, during braking, the pad surface can reach temperatures up to several hundred ºC on localised friction spots, the degradation of the binder may occur, accompanied by a reduction of the brake system stopping capability and by a significant increase in the wear rate. This phenomenon, known as fading, contributes to mass loss due to degradation of the methylene and phenol groups (Menapace et al., 2019). Thermal degradation of phenolic resins has already been documented in previous studies (Kukutschová et al., 2011). Some of the phenolic compounds detected are derived from lignin (e.g. vanillin). Recently, lignin polymers started to be applied in the formulations of automobile brake pads as binder and filler materials (Kumar and Kumaran, 2020; Park et al., 2020). Oxidised irgafos 168 [tris(2,4-di-tert-butylphenyl)phosphite] was present in the brake wear samples. It is an organophosphorus compound widely used as stabiliser in polymers with the role of acting as antioxidant or with other functions. The compound is a phosphite ester derived from di-tert-butylphenol. Bisphenol A, another constituent of PM_{10} samples, is employed as a stabiliser in brake fluids, thereby enhancing both useful life and durability.

Since the use of asbestos material is being avoided to manufacture brake pads as it is harmful and toxic in nature, diverse natural fibres have been employed as alternative products in reinforcing the friction composites. The components of natural fibres include cellulose, hemicelluloses, lignin, pectin, waxes and water soluble substances (Pujari and Shikiran, 2019). Studies of thermal stability and degradation of brake pads using thermogravimetric analysis (TGA) revealed that the decomposition temperatures vary greatly with formulations. Weight loss at about 330-350 ºC is generally observed due to thermal depolymerisation of hemicellulose and the cleavage of glucosidic linkages of cellulose (Gbadeyan, 2017; Kumar and Kumaran, 2020), leading to the formation of levoglucosan and other compounds usually described as products of biomass combustion (Vicente and Alves, 2018). However, the incorporation of carbon-carbon in the resin-matrix gives significant improvement to the thermal stability of the material and shifts of the weight loss towards higher temperatures may occur (Gbadeyan, 2017). Among the compounds resulting from the possible thermal degradation of natural fibres detected in the samples are some sugars and sterols (e.g. sitosterol and stigmasterol).

The differences in composition and concentrations could be attributed to diverse quantities and types of organic compounds used in the various commercial formulations and also to variable conditions applied in the “post-curing” phase of manufacturing. However, it should be borne in mind that organic materials (phenolic resins, graphite, fibres) undergo a thermal degradation which could also be catalysed by extreme localised pressures and the presence of catalysts, principally metals and their compounds (Křístková et al., 2004). Copper and iron exert a role as catalysts at higher temperatures, inducing the formation of radicals, which control further oxidation reactions. Metal oxides can also catalyse oxidation of functional groups (Křístková et al., 2004). Since during the braking process an oxidative atmosphere is expected, above certain temperature ranges, organic composites decompose, leading to the release of a multitude of both gas- and particulate phase

compounds (Kukutschová et al., 2010; Malachova et al., 2016). Due to the fact that friction materials are multicomponent composites, in most cases with confidential compositions, and because during braking very complex chemical and mechanical processes take place, it is very difficult to establish emission patterns and generalise organic profiles of particulate matter resulting from wear.

Table 3. Particulate mass fractions of phenolic compounds (μg g^{-1} PM_{10}) for different brake pads and test protocols (empty cells stand for not detected or below the detection limit).

Braking cycle	120-80 kph	200-170 kph	120-80 kph	200-170 kph	120-80 kph	200-170 kph	120-80 kph	FADE
Brake pad	NAO 1	NAO 1	NAO 2	NAO 2	Low steel 1	Low steel 1	Low steel 2	Low steel 2
Pyrocatechol	2.07	0.899	1.54	0.0132	0.448	0.448	0.157	0.662
5-Isopropyl-3-methylphenol	11.4	10.6	50.9	3.99	3.98	6.44	5.00	2.91
Resorcinol	0.147	0.357	3.20	0.492	0.318	0.798	0.470	0.0940
Eugenol	0.580	0.172	1.39	0.156	0.117	0.215	0.0975	0.085
Vanillin		26.5	95.8	7.96	21.0	21.0	24.2	7.04
Vanillic acid		1.04	22.1	5.41	0.318	3.57	0.282	2.09
2,4-di-tert-butylphenol	3733	1541	1042.9	1458	883	1545	23.6	854
4-tert-butylphenol	14.6	52.7	1456	360	5.06	237		68.9
Pyrogallol	0.189	0.0525	0.106	0.0484	0.0435	0.0612	0.0509	0.0212
Isoeugenol	7.72	68.5	14.7	1.26	2.09	3.13	2.77	0.650
4-Phenylphenol			0.207	0.792		0.279	0.0552	
Benzyl alcohol	932	531	13280	602	297	548		503
Benzoic acid	21.0	63.2	541	75.4	11.5	51.8	435	158
4-Hydroxybenzoic acid			61.4	9.89		5.30	3.97	3.33
Phenol, 2,4-bis(1,1-dimethylethyl)-	210	42.2	541	362		244	108	
Hydrocinnamic acid methyl ester		295						
Trans-cinnamic acid			69.2	21.3	36. 6	2.52		3.36
Phloretic (hydro-p-coumaric) acid		19.1	190	32.6	3.01		11.4	16.9
4-Hydroxy-3-methoxycinnamic (ferulic) acid					0.721	0.0356		0.176
Sinapyl alcohol					0.815	1.42		0.609
Bisphenol A	68.0		60.6		87.5	93.5		17.9
Oxidised irgafos 168	20321					2779		1518
Sum	25322	2658	26818	2941	1317	5544	615	3158

Conclusions

~~Understanding the sources that are harmful to health can provide valuable information for risk management strategies and could help decision-makers to develop more targeted air pollution regulation. Nowadays, it is known that non-exhaust emissions, which include brake wear particles, are one of the main causes that contribute to degradation of air quality, especially in urban environments. As these emissions are not regulated, few studies have addressed their physico-chemical properties, although projections indicate an increase in the coming years. Obtaining chemical emission profiles is essential not only to assess possible health effects, but also to apply source apportionment models to accurately quantify the different contributions to the atmospheric levels measured at receptor locations.~~

The few studies on particulate matter emissions from brake wear have been extremely focused on the metallic composition. As far as we know, the present study is one of the first attempts of gathering a comprehensive organic characterisation of the thoracic fraction of wear particles from different brake pads (two low steel and two non-asbestos organic).

Due to the complex chemomechanical interactions on the friction material surface, it is difficult to predict the brake performance and its wear emissions. In general, smaller PM_{10} levels and total carbon mass fractions were obtained during the test protocols with less braking and lower temperatures. The chromatographically resolved organic fraction encompassed more than 150 compounds. PM_{10} mass fractions of alkanes and alkenes were one order of magnitude lower for the test protocol with more severe braking and higher temperatures and pressures. Irrespective of the brake pads or testing cycles, a carbon preference index around 1, consonant with oil products, was obtained for n-alkanes. Only trace amounts of PAHs were found with total absence of high molecular weight compounds. Much higher amounts of n-alkanols were detected in PM_{10} from both non-asbestos organic brake pads. n-Alkanoic acids, diacids, plasticisers, phenol derivatives and glycol/glycerol related compounds were present in higher mass fractions in the PM_{10} resulting from the wear of one of the non-asbestos organic pads, especially during the smoothest braking cycle. Although some of the brake pads were grouped into the same category, completely different emissions suggest that they could contain significantly different organic materials. On the other hand, the same pad subjected to different braking circuits can generate quantitative and qualitatively different emissions due to divergent thermal and oxidative processes, some of which are catalysed by metallic constituents. Many of the detected organic compounds can be associated with components of brake formulations (e.g. phenolic resins, natural fibres, hydraulic fluids, etc.).

Despite the extensive database obtained, there is still a long way to go when it comes to the organic characterisation of brake wear particles. Bearing in mind the complexity and variety of commercial formulations, as well as the interactions that involve physical, chemical and mechanical

aspects during the various braking cycles, this work should be regarded as preliminary and as a motivating example for subsequent investigations, covering other categories of brakes. Since only a small fraction of the organic content of wear particles can be chromatographically resolved, investments should be made in the future in other techniques, or a combination of techniques, to increase the range of identified and quantified compounds.

Credit authorship contribution statement

Célia Alves: Conceptualisation, Supervision, Funding acquisition, Project administration, Formal analysis, Writing - Original draft preparation. **Margarita Evtyugina**: Methodology, Writing – Review & Editing. **Ana Vicente**: Methodology, Writing – Review & Editing. **Eleonora Conca**: Methodology, Writing – Review & Editing. **Fúlvio Amato**: Conceptualisation, Funding acquisition, Project administration, Writing – Review & Editing.

Declaration of competing interest

The authors declare that they have no known competing financial interests or personal relationships that could have appeared to influence the work reported in this paper.

Acknowledgments

The authors are grateful to the BBVA foundation (Ayudas a Investigadores y Creadores Culturales 2016), the POHP/FSE programme and the Portuguese Foundation of Science and Technology (FCT) for funding the scholarship SFRH/BPD/123176/2016. Ana Vicente was subsidised by national funds (OE), through FCT, I.P., in the framework contract foreseen in the numbers 4, 5 and 6 of article 23, of the Decree-Law 57/2016, of August 29, changed by Law 57/2017, of July 19. An acknowledgment is also due for the support to CESAM (UIDB/50017/2020+UIDP/50017/2020), to FCT/MCTES through national funds, and the co-funding by the FEDER, within the PT2020 Partnership Agreement and COMPETE2020. Chemical analyses were supported by the "Chemical and toxicological SOurce PROfiling of particulate matter in urban air (SOPRO)", POCI-01-0145-FEDER-029574, funded by FEDER, through COMPETE2020 - Programa Operacional Competitividade e Internacionalização (POCI), and by national funds (OE), through FCT/MCTES.

Appendix A. Supplementary data

Supplementary data to this article can be found online at https://doi. org/XXX

References

Alves, C.A., Vicente, A., Monteiro, C., Gonçalves, C., Evtyugina, M., Pio, C., 2011. Emission of trace gases and organic components in smoke particles from a wildfire in a mixed evergreen forest in Portugal. Sci. Total Environ. 409, 1466-1475.

Alves, C.A., Vicente, A.M.P., Calvo, A.I., Baumgardner, D., Amato, F., Querol, X., Pio, C., Gustafsson, M., 2020b. Physical and chemical properties of non-exhaust particles generated from wear between pavements and tyres. Atmos. Environ. 224, 117252. https://doi.org/10.1016/j.atmosenv.2019.117252

Alves, C.A., Vicente, E.D., Vicente, A.M.P., Casotti Rienda, I., Tomé, M., Querol, X., Amato, F., 2020a. Loadings, chemical patterns and risks of inhalable road dust particles in an Atlantic city in the north of Portugal. Sci. Total Environ. 737, 139596. https://doi.org/10.1016/j.scitotenv.2020.139596

Alves, C.A. Evtyugina, M., Vicente, A.M.P., Vicente, E.D., Nunes, T.V., Silva, P.M.A., Duarte, M.A.C, Pio, C.A., Amato, F., Querol, X., 2018. Chemical profiling of PM_{10} from urban road dust. Sci. Total Environ. 634, 41-51.

Amato, F., Alastuey, A., Karanasiou, A., Lucarelli, F., Nava, S., Calzolai, G., Severi, M., Becagli, S., Gianelle, V.L., Colombi, C., Alves, C., Custodio, D., Nunes, T., Cerqueira, M., Pio, C., Eleftheriadis, K., Diapouli, E., Reche, C., Minguillon, M.C., Manousakas, M.I., Maggos, T., Vratolis, S., Harrison, R.M., Querol, X., 2016. AIRUSE-LIFE plus: a harmonized PM speciation and source apportionment in five southern European cities. Atmos. Chem. Phys. 16, 3289-3309.

Barosova, H., Chortarea, S., Peikertova, P., Clift, M.J.D., Petri-Fink, A., Kukutschova, J., Rothen-Rutishauser, B., 2018. Biological response of an in vitro human 3D lung cell model exposed to brake wear debris varies based on brake pad formulation. Arch. Toxicol. 92, 2339-2351.

Blau, P.J., 2001. Compositions, Functions, and Testing of Friction Brake Materials and Their Additives. Report ORNL TM-2001/64, Oak Ridge National Lab., TN, United States. https://doi.org/10.2172/788356

Ciudin, R., Verma, P.C., Gialanella, S., Straffelini, G., 2014. Wear debris materials from brake systems: environmental and health issues. In: The Sustainable City IX, Vol. 2., Marchettini et al. (Eds), WIT Transactions on Ecology and The Environment. Southampton, UK. https://doi.org/10.2495/SC141202

Cui, Y., Cao, W., Ji, D., Gao, W., Wang, Y., 2021. Estimated contribution of vehicular emissions to carbonaceous aerosols in urban Beijing, China. Atmos. Res. 248, 105153. https://doi.org/10.1016/j.atmosres.2020.105153

Dale, E., Trim, H., 2017. Phthalates in exterior use products – existing data summary. Zero Waste Washington, USA.

DEFRA, 2019. Non-Exhaust Emissions from Road Traffic. Air Quality Expert Group's Report. Department for Environment Food & Rural Affairs. United Kingdom.

Eze, C.C., 2016. Formulation and production of bio-hydraulic fluid as an alternative to mineral fluids for automobiles. Am. J. Eng. Res. 5, 147-151.

FAT, 2017. The Contribution of Brake Wear Emissions to Particulate Matter in Ambient Air. Forschungsvereinigung Automobiltechnik e.V., Berlin, Germany.

Fromme, H., Mi, W., Lahrz, T., Kraft, M., Aschenbrenner, B., Bruessow, B., Ebinghaus, R., Xie, Z., Fembacher, L., 2018. Occurrence of carbazoles in dust and air samples from different locations in Germany. Sci. Total Environ. 610-611, 412-418.

Gadd, J., Kennedy, P., 2000. Preliminary examination of organic compounds present in tyres, brake pads and road bitumen in New Zealand. Prepared for the Ministry of Transport by Kingett Mitchell Limited.

Garg, B.D., Cadle, S.H., Mulawa, P.A., Groblicki, P.J., 2000. Brake wear particulate matter emissions. Environ. Science Technol. 34, 4463-4469.

Gasser, M., Riediker, M., Mueller, L., Perrenoud, A., Blank, F., Gehr, P., Rothen-Rutishauser, B., 2009. Toxic effects of brake wear particles on epithelial lung cells *in vitro*. Part. Fibre Toxicol. 6, 30. https://doi.org/10.1186/1743-8977-6-30

Gbadeyan, O.J., 2017. Low friction hybrid nanocomposite material for brake pad application. Master in Mechanical Engineering. Faculty of Engineering and the Built Environment, Durban University of Technology.

Gerlofs-Nijland, M.E., Bokkers, B.G.H., Sachse, H., Reijnders, J.J.E., Gustafsson, M., Boere, A.J.F., Fokkens, P.F.H., Leseman, D.L.A.C., Augsburg, K., Cassee, F.R., 2019. Inhalation toxicity profiles of particulate matter: a comparison between brake wear with other sources of emission. Inhal. Toxicol. 31, 89-98.

Grigoratos, T., Martini, G., 2015. Brake wear particle emissions: a review. Environ. Sci. Pollut. Res. 22, 2491–2504.

Gudmand-Høyer, L., Bach, A., Nielsen, G.T., Morgen, P., 1999. Tribological properties of automotive disc brakes with solid lubricants. Wear 232, 168-175.

Hagino, H., Oyama, M., Sasaki, S., 2016. Laboratory testing of airborne brake wear particle emissions using a dynamometer system under urban city driving cycles. Atmos. Environ. 131, 269-278.

Harrison, R.M., Jones, A.M., Gietl, J., Yin, J., Green, D.C., 2012. Estimation of the contributions of brake dust, tire wear, and resuspension to nonexhaust traffic particles derived from atmospheric measurements. Environ. Sci.Technol. 46, 6523-6529.

Hussain, S., Abdul Hamid, M.K., Mat Lazim A.R., Abu Bakar, A.R., 2014. Brake wear particle size and shape analysis of non-asbestos organic (NAO) and semi metallic brake pad. J. Teknol. 71, 129-134.

Iijima, A., Sato, K., Yano, K., Kato, M., Kozawa, K., Furuta, N., 2008. Emission factor for antimony in brake abrasion dust as one of the major atmospheric antimony sources. Environ. Sci. Technol. 42, 2937-2942.

Iijima, A., Sato, K., Yano, K., Kato, M., Tago, H., Kato, M., Kimura, H., Furuta, N., 2007. Particle size and composition distribution analysis of automotive brake abrasion dusts for the evaluation of antimony sources of airborne particulate matter. Atmos. Environ. 41, 4908-4919.

Kazimirova, A., Peikertova, P., Barancokova, M., Staruchova, M., Tulinska, J., Vaculik, M., Vavra, I., Kukutschova, J., Filip, P., Dusinska, M., 2016. Automotive airborne brake wear debris nanoparticles and cytokinesis-block micronucleus assay in peripheral blood lymphocytes: A pilot study. Environ. Res. 148, 443-449.

Křístková, M., Filip, P.,Weiss, Z., Peter, R., 2004. Influence of metals on the phenol formaldehyde resin degradation in friction composites. Polym. Degrad. Stab. 84, 49-60.

Kukutschová, J., Moravec, P., Tomášek, V., Matějka, V., Smolík, J., Schwarz, J., Seidlerová, J., Šafářová, K., Filip, P., 2011. On airborne nano/microsized wear particles released from low-metallic automotive brakes. Environ. Pollut. 159, 998-1006.

Kukutschová, J., Roubíček, V., Mašláň, M., Jančík, D., Slovák, V., Malachová, K., Pavlíčková, Z., Filip, P., 2010. Wear performance and wear debris of semi-metallic automotive brake materials. Wear 268, 86-93.

Kumar, V.V., Kumaran, S.S., 2020. Characterization of various properties of chemically treated *Allium sativum* fiber for brake pad application. J. Nat. Fibers. https://doi.org/10.1080/15440478.2020.1745130

Malachova, K., Kukutschova, J., Rybkova, Z., Sezimova, H., Placha, D., Cabanova, K., Filip, P., 2016. Toxicity and mutagenicity of low-metallic automotive brake pad materials. Ecotoxicol. Environ. Saf. 131, 37-44.

Mamakos, A., Arndt, M., Hesse, D., Augsburg, K., 2019. Physical characterization of brake-wear particles in a PM_{10} dilution tunnel. Atmosphere 10, 639. https://doi.org/ 10.3390/atmos10110639

Menapace, C., Leonardi, M., Secchi, M., Bonfanti, A., Gialanella, S., Straffelini, G., 2019. Thermal behavior of a phenolic resin for brake pad manufacturing. J. Therm. Anal. Calorim. 137, 759–766.

Menapace, C., Mancini, A., Federici, M., Straffelini, G., Gialanella, S., 2020. Characterization of airborne wear debris produced by brake pads pressed against HVOF-coated discs. Friction 8, 421-432.

Mosleh, M., Blau, P.J, Dumitrescu, D., 2004. Characteristics and morphology of wear particles from laboratory testing of disc brake materials. Wear 256, 1128-1134.

Mukherjee, A., Agrawal, M., 2018. Assessment of local and distant sources of urban $PM_{2.5}$ in middle Indo-Gangetic plain of India using statistical modelling. Atmos. Res. 213, 275-287.

Park, J., Hwang, H., Kim, J.Y., Choi, J.W., 2020. Applicability of lignin polymers for automobile brake pads as binder and filler materials and their performance characteristics. Environ. Technol. 41, 488-497.

Pujari, S., Srikiran, S., 2019. Experimental investigations on wear properties of Palm kernel reinforced composites for brake pad applications. Def. Technol. 15, 295-299.

Ramdahl, T. 1983. Retene - a molecular marker of wood combustion in ambient air. Nature 306, 580-582.

Rogge, W.F., Hildemann, L.M., Mazurek, M.A., Cass, G.R., Simoneit, B.R.T., 1993. Sources of fine organic aerosol. 3. Road dust, tire debris, and organometallic brake lining dust: roads as sources and sinks. Environ. Sci.Technol. 27, 1892-1904.

Sanders, P.G., Xu, N., Dalka, T.M., Maricq, M.M., 2003. Airborne brake wear debris: Size distributions, composition, and a comparison of dynamometer and vehicle tests. Environ. Sci.Technol. 37, 4060-4069.

Selley, L., Schuster, L., Marbach, H., Forsthuber, T., Forbes, B., Gant, T.W, Sandström, T., Camiña, N., Athersuch, T.J., Mudway, I., Kumar, A., 2020. Brake dust exposure exacerbates inflammation and transiently compromises phagocytosis in macrophages. Metallomics 12, 371. https://doi.org/10.1039/c9mt00253g

Sokolski, P., Sokolska, J., 2019. Assessment of the influence of the coefficient of friction on the temperature distribution of a disk brake during the braking process. Tribologia 6, 95-99.

Thorpe, A, Harrison, RM, 2008. Sources and properties of non-exhaust particulate matter from road traffic: a review. Sci. Total Environ. 400, 270-282

Wahlström, J., Olander, L., Olofsson, U., 2010. Size, shape, and elemental composition of airborne wear particles from disc brake materials. Tribol. Lett. 38, 15-24.

Xiao, X., Yin, Y., Bao, J., Lu, L., Feng, X., 2016. Review on the friction and wear of brake materials. Adv. Mech. Eng. 8, 1-10.

Zhao, J., Lewinski, N., Riediker, M., 2015. Physico-chemical characterization and oxidative reactivity evaluation of aged brake wear particles. Aerosol Sci. Tech. 49, 65-74.

Supplementary data

Table S1. Particulate mass fractions of organic compounds (μg g^{-1} PM_{10}) for different brake pads and test protocols (empty cells stand for not detected or below the detection limit).

Braking cycle	120-80 kph	200-170 kph	120-80 kph	200-170 kph	120-80 kph	200-170 kph	120-80 kph	FADE
Brake pad	NAO 1	NAO 1	NAO 2	NAO 2	Low steel 1	Low steel 1	Low steel 2	Low steel 2
n-Alkanes								
Undecane						8.62		
Dodecane	29.8	26.2			5.54		4.51	3.78
Tridecane	64.5	15.0	34.7		9.04	5.14	59.6	3.69
Tetradecane	14.9	3.61	73.6		6.49	41.7		1.21
Pentadecane			100			582	23.4	
Hexadecane	20.2		53	30.1	2.67	155	54.3	
Heptadecane	87.1	10.7	4 86	106	5.11	1577	161	1.16
Octadecane	25.9		1053	190	5.94	234	237	0.717
Nonadecane			1027	171		243	194	
Eicosane	32 2	1.09	1075	158	26.8	259	220	1.92
Heneicosane	20.0	408	1203	214	41.1	409	223	4.69
Docosane	135	17.5	1888	298	107	451	371	11.1
Tricosane	47.1		2595	345	131	644	570	3.82
Tetracosane	5.56		5036	846	296	1091	1159	
Pentacosane	25.9		6154	958	428	1336	1423	
Hexacosane	406		10075	1180	652	2253	1741	
Heptacosane	102	8230	6018	962	603	1266	1540	
Octacosane	3615	235	7573	699	625	1520	1507	
Nonacosane	371		6578	581	522	1450	1239	3.00

Triacontane	298		6070	449	421	1372	1115	
Hentriacontane					462		770	19.8
Dotriacontane			3981		185	884	409	7.71
Tritriacontane	4506		1798			458	175	
Σ n-Alkanes	9816	8950	68053	7186	4535	16238	13194	62.5
Alkenes								
Dodecene								
Tetradecene	40.6		75.2		3.81	39.5		2.31
Hexadecene	41.6		380	34.3	4.60	98.3	50.3	
Octadecene	127	18.5	312	75.1	16.8	61.0	115	
Nonadecene							58.8	
Eicosadiene			474					
Eicosene	89.0	17.0			15.0		38.5	3.6
Nonadecene								
Docosene								
Tricosene				78.2	27.8		68.7	7.3
Σ Alkenes	299	35.5	142	188	67.9	199	331	13.2
Cycloalkanes								
Cyclohexadecane			112			30.1	6.90	
Cyclopentadecane						86.4		
Branched aliphatics								
Phytane	27.1			85.6	2.53		126	0.902
Pristane			321	45.7		94.2	44.2	5.53
3-methyl-heptadecane						47.4	29.3	
Squalene								
Alkanols	0.423	1.19	115	9.41	0.577	10.9	0.169	0.592
Decanol	261	27.6	447	86.5	12.5	55.8	0.437	23.6
Dodecanol	247	17.8	152	258	20.7	228	1.89	11.6
C_{14} alcohol (tetradecanol or methyl	50.6	53.7	264	1124	223	1947		

tridecanol)								
Pentadecanol	508	116	307	430	208	592	106	58.9
Hexadecanol	42.9		93.1	365		331		
Heptadecanol	2659	1499	5147	989	1210	1496	182	380
Octadecanol		108	3942	1622	430	1755		176
Eicosanol	592	122		219	170		4.13	
Docosanol	10.5	2.01	21.9	13.2	2.18	5.84	1.65	0.423
Pentacosanol	11.0	3.57	8.05	1.88	2.41	3.70	1.75	0.458
Heptacosanol	76.2	20.47	52.9	7.68	17.7	19.0	3.17	5.51
Octacosanol	21.2	4.29	12.5	2.39	6.30	5.83	1.04	2.34
Tricontanol	0.423	1.19	115	9.41	0.577	10.9	0.169	0.592
Decanol	261	27.6	447	86.5	12.5	55.8	0.437	23.6
Σ Alkanols	4479	1976	10563	5127	2303	6450	306	659
n-Alkanoic acids								
Octanoic (caprylic) acid	59.8	58.1	774	64.8	29.2	48.0	61.6	61.6
Nonanoic (pelargonic) acid	144	142	1524	174	113	212	191	142
n-decanoic (caproic) acid	413	180	3665	329	222	366	153	101
Undecanoic acid			61.1	11.7		53.6	3.42	7.59
Dodecanoic (lauric) acid	56.0	290	1900	1093	108	845	267	121
Tridecanoic acid		1.62	134	214	1.72	174	39.4	21.1
Tetradecanoic (myristic) acid	212	660	4779	1638	307	2205	712	578
Pentadecanoic acid		229	1193	699	106	798	197	119
Hexadecanoic (palmitic) acid	3000	5465	11923	5091	2812	6630	6756	827
Heptadecanoic acid		120	1760	473	45.3	566	138	207
Octadecanoic (stearic) acid		7259	15535	3819	2809	4667	4194	1955
Nonadecanoic acid		13.8		13.3	2.63	18.4	7.50	8.17
Eicosanoic (arachidic) acid		59.8	512	78.5	7.68	102	42.2	43.6
Docosanoic (behenic) acid		28.3	361	62.8		53.0	30.8	22.4
Σ n-Alkanoic acids	3884	14507	43820	13761	6562	16739	12794	4216

Alkenoic acids								
Palmitoleic		31.5	377	37.2	0.712	11.0	111	25.3
Palmitelaidic	84.8	27.3	242				44.3	
Oleic	114	84.9	694	76.6	34.9	108	139	42.0
Linoleic		6.62	101	12.9	0.340	11.7	0.427	5.29
Margaroleic			477	94.2		130		
Elaidic			360	76.2		165		
Σ Alkenoic acids	199	150	2251	297	35.9	425	293	72.6
Dicarboxylic acids								
Ethanedioic (oxalic) acid		1019	11869	2174			3970	80.3
Butanedioic (succinic) acid		161	2754	834		83.9		140
Hexanedioic (adipic) acid			3242	613		148		118
Heptanedioic (pimelic) acid			260	56.1		16.1	3.50	15.9
Octanedioic (suberic) acid			356	162		18.4		39.7
Nonanedioic (azelaic) acid			312	319		41.6		96.8
Decanedioic (sebacic) acid		2.28	93.6	37.8		13.3	0.765	8.42
Σ Dicarboxylic acids		1182	18883	4196		326	3974	499
Other acids								
Glycolic acid		631	2108	204		107	1846	4.11
Pyruvic acid		702	4902	1052		891	1161	436
Levulinic acid		390	3861	435	431	113		461
3-Hydroxypropanoic acid			1140	352		475	583	114
2,3-Dihydroxy-2-methylpropanoic acid		112	2004	300		565	496	192
3,4-Dihydroxybutanoic acid		141	1576	347		475	68.0	227
3-hydroxybutanoic ((R)-3-hydroxybutyric) acid			365	128			393	
Cis-Pinonic acid			237	72.6		41.3	24.4	43.4
Pinic acid			201	19.7		16.0	3.37	10.0
Citric acid		1.36	46.6	30.0	0.275	4.15	0.0900	5.49
Dehydroabietic acid		8.28	36.9	7.22	0.994	7.51	6.16	3.01

Σ Other acids		2015	16475	2947	432	2695	4582	1497
Plasticisers								
Tributyl acetylcitrate	1048	653		5.67	877	329		
Diisooctyl adipate	2775	687	25050	554	374	387		47.5
Diethyl phthalate	484	13.3	940	51.6		454	4.53	168
Di-n-butyl phthalate	1204	97.7	571	234	95.4	363	67.7	352
Bis(2-ethylhexyl)phthalate	80.2			1208	988	3641		
Bis(2-ethylhexyl)adipate	951	418			383	1793	[illegible]	256
Dimethyl phthalate			0.367	0.470	0.253	0.552		0.147
Di-n-octyl phthalate		1272						
Σ Plasticisers	6542	3141	26561	2054	2717	6367	113	824
Glycol/glycerol related compounds								
Glycerol	91.8	53.8	12761	2407	136	1199	4157	712
Glyceric acid		47.3	5420	942		332	59.7	429
1-monolauroyl-rac-glycerol	0.286	0.149	0.601	6.08	0.170	0.314	1.12	0.0281
2-[2-(2-methoxyethoxy)ethoxy]ethanol		40.8	4302	1233	45.4	614	377	689
2-[2-(2-ethoxyethoxy)ethoxy]ethanol		24.4	879	1964	99.0	1598	92.2	215
1-Monomyristin								
1-Monopalmitin			4257	284	57.2	993	141	377
Monostearin		245	2634	641	101	594	808	
1,3-dipalmitin	400			302	124		527	21.6
Σ Glycol/glycerol related compounds	492	411	39448	7852	562	5495	6208	2467
Other compounds								
Levoglucosan							26.2	
Galactosan				5.06			7.05	
D-glucuronic acid lactone			129	48.2		25.4	39.9	14.4
Quebrachitol	0.649	0.166	0.795	0.114	0.172	0.0271	0.280	0.160
Unidentified sugars		1.28	862	225		49.3	81.6	29.0
Cholesterol	725	291	716	62.2	278	132	36.8	83.6

5-Cholesten-3-ol (dihydrocholesterol)	40.8			5.61	7.06			
Stigmasterol			84.9	13.3		32.0		
b-Sitosterol	128	81.9	1188	129	75.0	275		13.0
1,2,3-Hexanetriol	0.297	0.135	2.41	0.381	0.127	0.193	0.128	0.0527
2,6-Di-tert-butylbenzoquinone	1315	617	2504	853	426	275	35.7	113
7,9-Di-tert-butyl-1-oxaspiro[4.5]deca-6,9-diene-2,8-dione	2401	337	2240	230	373	472		199
L-5-oxoproline			6017	1266		79.6		
1,2-Benzenedicarboxylic acid, dibutyl ester	11.7				4.95			70.2

Table S2. Relationships between individual n-alkanes (x, μg g^{-1} PM_{10}) and total n-alkanes (y, mg g^{-1} PM_{10}) in the 8 samples listed in Table 1. Only correlations with r^2>0.7 are shown.

n-Alkane	Linear relationship	r^2
C_{20}	y=0.0565x+5.4664	0.7893
C_{21}	y=0.0536x+0.4084	0.8863
C_{22}	y=0.0342x+3.8076	0.8516
C_{23}	y=0.0252x+3.4327	0.9207
C_{24}	y=0.0129x+2.9949	0.9304
C_{25}	y=0.0102x+2.3211	0.9566
C_{26}	y=0.0058x+2.8489	0.9428
C_{28}	y=0.0078x+0.6096	0.8732
C_{29}	y=0.0097x+2.1938	0.9751
C_{30}	y=0.0106x+2.3122	0.9742
C_{32}	y=0.0160x+4.3013	0.9178

Table S3. Interrelationships between individual PAH (μg g^{-1} PM_{10}) and with total PAH (μg g^{-1} PM_{10}) in the 8 samples listed in Table 1. Only correlations with r^2>0.7 are shown.

x	y	Linear equation	r^2
acenaphthene	fluorene	y=6.552x-0.7683	0.9195
acenaphthene	phenanthrene	y=0.9343x-0.2271	0.7947
acenaphthene	retene	y=0.7008x+0.5562	0.7060
acenaphthene	chrysene	y=0.2842x-0.1376	0.7447
fluorene	phenanthrene	y=0.1352x+0.0079	0.7767
fluorene	pyrene	y=0.0648x+0.9769	0.7159
fluorene	retene	y=0.1030x+0.7048	0.7125
fluorene	chrysene	y=0.0441x-0.1157	0.8354
phenanthrene	fluoranthene	y=0.3242x+0.766	0.8319
phenanthrene	retene	y=0.7657x+0.6908	0.9258
phenanthrene	chrysene	y=0.2732x+0.0027	0.7559
fluoranthene	retene	y=1.9493x+0.4589	0.7580
retene	chrysene	y=0.3337x-0.1872	0.7140
acenaphthene	total PAHs	y=10.177x+1.6906	0.9398
fluorene	total PAHs	y=1.5202x+3.4455	0.9790
phenanthrene	total PAHs	y=9.3501x+7.709	0.8713
pyrene	total PAHs	y=17.357x-6.8103	0.7481

retene	total PAHs	y=11.337x+1.4151	0.8112
chrysene	total PAHs	y=29.504x+10.58	0.8568

Table S4. Relationships between individual n-alkanoic acids (x, μg g^{-1} PM_{10}) and total n-alkanoic (y, mg g^{-1} PM_{10}) in the 8 samples listed in Table 1. Only correlations with r^2>0.7 are shown.

n-Alkanoic acid	Linear relationship	r^2
C_9	y=0.0279x+6.5625	0.8036
C_{10}	y=0.0119x+8.2333	0.7603
C_{12}	y=0.0202x+4.2761	0.7852
C_{14}	y=0.0056x+3.8206	0.8777
C_{16}	y=0.0036x-3.2299	0.8783
C_{17}	y=0.0195x+5.2823	0.9105
C_{18}	y=0.0026x+1.6413	0.9439
C_{20}	y=0.0773x+7.1435	0.9221
C_{22}	y=0.1073x+6.8585	0.9015

Table S5. Interrelationships between individual n-alkanoic acids (μg g^{-1} PM_{10}) in the 8 samples listed in Table 1. Only correlations with r^2>0.7 are shown.

n-Alkanoic acids		Linear relationship	r^2
C_8	C_9	y=1.8972x+81.134	0.9765
	C_{10}	y=4.3137x+60.588	0.9787
	C_{20}	y=0.6732x+30.260	0.8770
	C_{22}	y=0.4890x+19.181	0.8532
C_9	C_{10}	y=2.2568x-111.80	0.9874
	C_{12}	y=1.1601x+193.66	0.7202
	C_{17}	y=2.9602x-258.65	0.9406
	C_{18}	y=10.045x+2205.8	0.7295
	C_{19}	y=0.1147x-8.7579	0.9554
	C_{20}	y=0.3616x+0.0667	0.9215
	C_{22}	y=0.2619x-3.2104	0.9019
C_{10}	C_{12}	y=0.5084x+255.07	0.7136
	C_{14}	y=4.1178x-132.76	0.8529
	C_{17}	y=1.3142x-108.12	0.8722
	C_{19}	y=0.0505x-2.7356	0.8707
	C_{20}	y=0.1570x+21.365	0.9013

	C_{22}	y=0.1141x+11.117	0.8832
C_{11}	C_{14}	y=64.837x+319.58	0.8664
	C_{15}	y=18.880x+126.52	0.7373
	C_{17}	y=21.804x+35.810	0.7281
C_{12}	C_{17}	y=0.9602x-6.227	0.7430
	C_{20}	y=0.2520x-29.90	0.7978
	C_{22}	y=0.1780x-17.72	0.7784
C_{13}	C_{15}	y=5.6124x+92.11	0.7577
C_{14}	C_{15}	y=0.2907x+34.343	0.8484
	C_{17}	y=0.3397x-78.293	0.9753
	C_{18}	y=2.3511x+1261.1	0.7832
	C_{19}	y=0.0118x-0.3731	0.9483
	C_{20}	y=0.0782x-27.585	0.8060
	C_{22}	y=0.0566x-18.820	0.8270
C_{15}	C_{17}	y=0.9420x+16.544	0.7487
	C_{19}	y=0.0300x+3.0302	0.7264
C_{16}	C_{18}	y=1.2778x-1196.0	0.7694
	C_{20}	y=0.0409x-100.0[illegible]	0.7340
C_{17}	C_{18}	y=7.0396x+1734.1	0.8308
	C_{19}	y=0.0377x+[illegible]	0.9615
	C_{20}	y=0.2401x-15.297	0.8989
	C_{22}	y=0.9218x-9.8993	0.9218
C_{18}	C_{19}	y=0.0047x-3.4698	0.8091
	C_{20}	y=0.0031x-56.562	0.8958
	C_{22}	y=0.0219x-36.212	0.8694
C_{19}	C_{20}	y=4.8178x-7.0656	0.9054
	C_{22}	y=3.6879x-6.6550	0.9496
C_{20}	C_{22}	y=0.7052x+3.5094	0.9730

Credit authorship contribution statement

Célia Alves: Conceptualisation, Supervision, Funding acquisition, Project administration, Formal analysis, Writing - Original draft preparation. **Margarita Evtyugina**: Methodology, Writing – Review & Editing. **Ana Vicente**: Methodology, Writing – Review & Editing. **Eleonora Conca**: Methodology, Writing – Review & Editing. **Fúlvio Amato**: Conceptualisation, Funding acquisition, Project administration, Writing – Review & Editing.

Declaration of competing interest

The authors declare that they have no known competing financial interests or personal relationships that could have appeared to influence the work reported in this paper.

Highlights

PM_{10} from wear of low steel and NAO pads were sampled for distinct braking cycles

Test protocols with less braking and lower temperatures generated lower PM_{10} levels

Total carbon decreased with the severity of the braking cycles

More than 150 organic compounds were detected in PM_{10}

Larger amounts of organic compounds were emitted by NAO pads under smooth braking